

Antisymmetric quadrupole mode of coherent structures in wall-bounded turbulence

Haiping Tian,¹ Shaoqiong Yang,¹ Lu Cheng,¹ Yuan Wang,¹ and Nan Jiang^{1,2,3, a)}

¹⁾ *Department of Mechanics, Tianjin University, Tianjin 300072, China*

²⁾ *Tianjin Key Laboratory of Modern Engineering Mechanics, Tianjin 300072, China*

³⁾ *State Key Laboratory of Nonlinear Mechanics, Institute of Mechanics, CAS, Beijing 100190, China*

(Received 3 July 2013; accepted 27 August 2013; published online 10 September 2013)

Abstract Experiments were conducted in a water tunnel by tomographic time-resolved particle image velocimetry (Tomo-TRPIV). The Reynolds number Re_θ is 2460 on the base of momentum thickness. According to the physical mechanism of the stretch and compression of multi-scale vortex structures in the wall-bounded turbulence, the topological characteristics of turbulence statistics in logarithmic layer were illustrated by local-averaged velocity structure function. During coherent structures bursting, results reveal that the topological structures of velocity gradients, velocity strain rates and vorticities behave as antisymmetric quadrupole modes. A three-layer antisymmetric quadrupole vortex packet confirms that there is a tight relationship between the outer layer and the near-wall layer. © 2013 The Chinese Society of Theoretical and Applied Mechanics. [doi:10.1063/2.1305202]

Keywords: wall-bounded turbulence, antisymmetric quadrupole mode, Tomo-TRPIV, vortex packet, coherent structure

In wall-bounded turbulent flows, the coherent structure burst is a kind of multi-scale quasi-periodic motion, which has spatial-temporal organized characteristics.^{1,2} In recent decades, many works focus on the investigation of the coherent structures dynamics with the aim to establish reasonable models of turbulence. After Falco³ found large scale motion (LSM) in turbulent boundary layers (TBLs), Head and Bandyopadhyay⁴ further pointed out that the LSM consists many hairpin vortices and they form a packet. Moin and Kim⁵ achieved the similar results from direct numerical stimulation (DNS). From then on, the focus of coherent structures study moves forward the vortex dynamics. In particular, Adrian et al.⁶ gave the idealized scheme of hairpin vortex packets which is growing up from the wall along the free-stream direction. Nevertheless, there is still a lack of a general model of coherent structures in turbulence.

The letter investigated the topological information around the ejection event in the logarithmic layer of the TBL. The three dimensional-three component (3D-3C) instant velocity vector fields of the TBL were measured by tomographic time-resolved particle image velocimetry (Tomo-TRPIV) in a water tunnel of Delft University of Technology. Then the spatial topological eigenmodes of the turbulence statistics, fluctuation velocities, vorticities, velocity gradients, and strain rates of velocity, were obtained.

The experiments were conducted in a water tunnel where a TBL flow has already developed along a flat plate which was vertical-mounted. Figure 1 is the schematic of the experimental arrangement. The free-coming stream velocity was 0.53 m/s. On the forepart of the acrylic glass plate, a spanwise attached band tripped the incoming flow and eventually generated a

TBL of 38 mm corresponding to $Re_\theta=2460$ on the base of the momentum thickness in measurement volume. The skin-friction velocity u_τ was 0.0219 m/s with accordingly the friction coefficient $c_f=0.00345$. A Tomo-TRPIV system has been utilized, containing two main parts. One is a diode-pumped laser with a high repetition and its maximum pulse energy is 25 mJ at 1 kHz; the other part is the image recording system with six cameras and its resolution is 1024 pixels \times 1024 pixels in full frame modus. The light was introduced perpendicular to the free-coming direction and parallel to the acrylic glass plate. The mean diameter of polyamide seeding particles is 56 μm . The light scattered by these particles was sufficient.

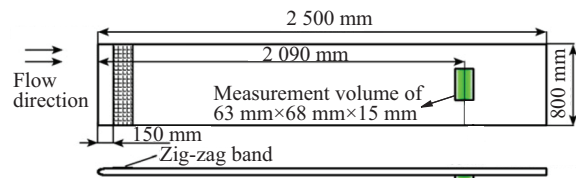


Fig. 1. Schematic of the experiment arrangement.

The measurement volume of about 63 mm (in streamwise) \times 68 mm (in spanwise) \times 15 mm (in wall-normal), was illuminated at 1 kHz frequency by the diode-pumped double high repetition rate laser. Meanwhile, five series of 2040 images were obtained during 10 s at the same sampling frequency. The DaVis7.3 software successively reconstructed 3D-3C velocity vector fields in time series. Eventually, a sequences of 3D-3C instant velocity vector volumes of 99 \times 99 \times 22 velocity vectors in the log-law region with spatial resolution of 0.687 mm (\sim 15 wall units) and 2 ms increment were obtained after errors were estimated. Since the complexity of the experimental system and the large amount of

^{a)}Corresponding author. Email: nanj@tju.edu.cn.

details to ensure the accuracy of the experiment, this letter just gives a simple description of the experiment. However, concrete details can be found in Ref. 7.

In present research of coherent structures, the local-averaged velocity structure function was proposed by Liu et al.⁸ Yang and Jiang⁹ extended it into a 3D spatial case which was defined as

$$\delta u_x(x_0, l) = \frac{\overline{u(x, y, z)_{x \in [x_0, x_0+l]}} - \overline{u(x, y, z)_{x \in [x_0-l, x_0]}}}{l}, \quad (1)$$

$$\delta u_y(y_0, l) = \frac{\overline{u(x, y, z)_{y \in [y_0, y_0+l]}} - \overline{u(x, y, z)_{y \in [y_0-l, y_0]}}}{l}, \quad (2)$$

$$\delta u_z(z_0, l) = \frac{\overline{u(x, y, z)_{z \in [z_0, z_0+l]}} - \overline{u(x, y, z)_{z \in [z_0-l, z_0]}}}{l}. \quad (3)$$

They indicate the local stretch-compressive (Eq. (1)), shear (Eq. (2)), or rotation (Eq. (3)) deformation at different scales of certain eddy structures in the turbulent flows, where u represents the velocity component in the streamwise, x_0 stands for the central position of the deformation along the streamwise with the similar interpretation for y_0 and z_0 , l represents the spatial certain scale of eddy structure, and $\overline{u(x, y, z)}$ stands for the locally averaged streamwise velocity in two neighboring eddies, and the centers of the two eddies were located at $x_0 + l/2$ and $x_0 - l/2$, respectively. For the spatial distribution of instantaneous fluctuation velocity in the wall-bounded turbulence, the coherent structure detection functions are expressed as

$$D(b; l) = \begin{cases} 1, & \delta u_x^-(b; l) < 0 \text{ and } \delta u_x^+(b; l) > 0, \\ 0, & \text{otherwise,} \end{cases} \quad (4)$$

where $D(b; l) = 1$ stands for the ejection motions. $\delta u_x^+(b; l) > 0$ indicated that the fluids in the downstream is stretched, while $\delta u_x^-(b; l) < 0$ means the upstream fluids is compressed. Taking the quasi-periodic repeatability of burst events into account, a phase-lock average scheme to extract the spatial topological eigenmodes of the coherent structure statistics was given as

$$\langle f(x; l_j) \rangle_e = \frac{1}{N_j} \sum_{i=1}^{N_j} f(b_i + x),$$

$$x \in \left[-\frac{l_j}{2}, \frac{l_j}{2} \right], \text{ while } D(b_i; l_j) = 1, \quad (5)$$

where $\langle \rangle$ represents the ensemble average, $f(x; l_j)$ represents the wondering component which could be the velocity fluctuation or the vorticity fluctuation, N_j represents the number of ejection or sweep events bursting with j -th scale, and l_j is the j -th scale of coherent structures.

The spatial locally averaged velocity structure functions were calculated by Eqs. (1)–(3). To obtain spatial

phase-average components of the velocity fluctuation, we firstly detect the burst event center which meets the condition criterion of Eq. (4). The rectangular volumes of $32\Delta x \times 32\Delta y \times 14\Delta z$ with $480 \times 480 \times 210$ wall units whose centers meet the condition criterion of Eq. (4) were segmented from the flow field with the wondering quantity. Then the components were extracted by phase averaging these rectangular volumes according to Eq. (5). Lastly, we analyze the spatial topologies of coherent structures from the spatial phase-lock average mode, where ejection bursting events happened in the bottom centers of these rectangular volumes. The dimensionless normal height of these volumes is from $z^+ = 135$ to $z^+ = 345$.

Figure 2 shows the velocity fluctuation vector field of ejection event with the contour of the velocity components in the streamwise (Fig. 2(a)) and wall-normal (Fig. 2(b)). The red spot in Fig. 2(a) represents the high-speed fluid while the blue spot in Fig. 2(a) shows the low-speed fluid. As can be seen from Fig. 2(b), the wall-normal fluctuating velocity is negative with the high-speed fluid, while it is positive which corresponds the low-speed fluid. This indicates that the high-speed fluids sweep down towards the wall while the low-speed fluids burst an ejection event in which fluids move to the opposite direction.

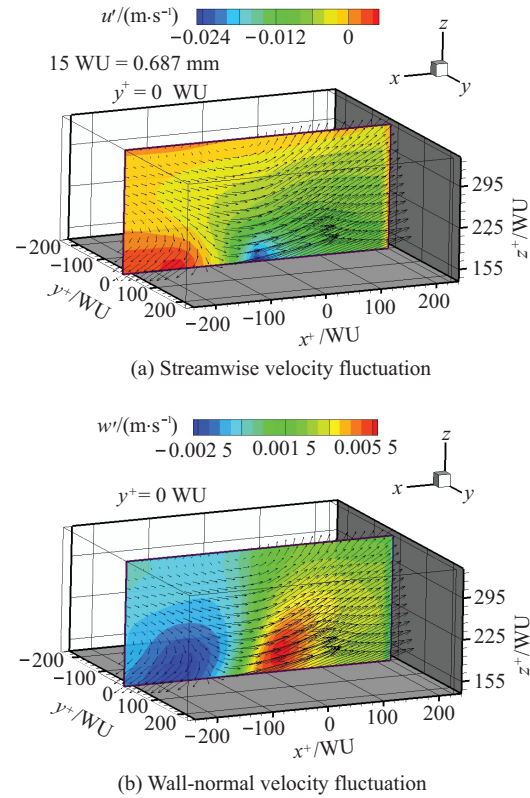


Fig. 2. Slices of velocity fluctuation vector field during ejection in the center of bottom.

Figure 3 is the iso-surface contours of streamwise vorticity components ω_1 . In Fig. 3(a), there are three

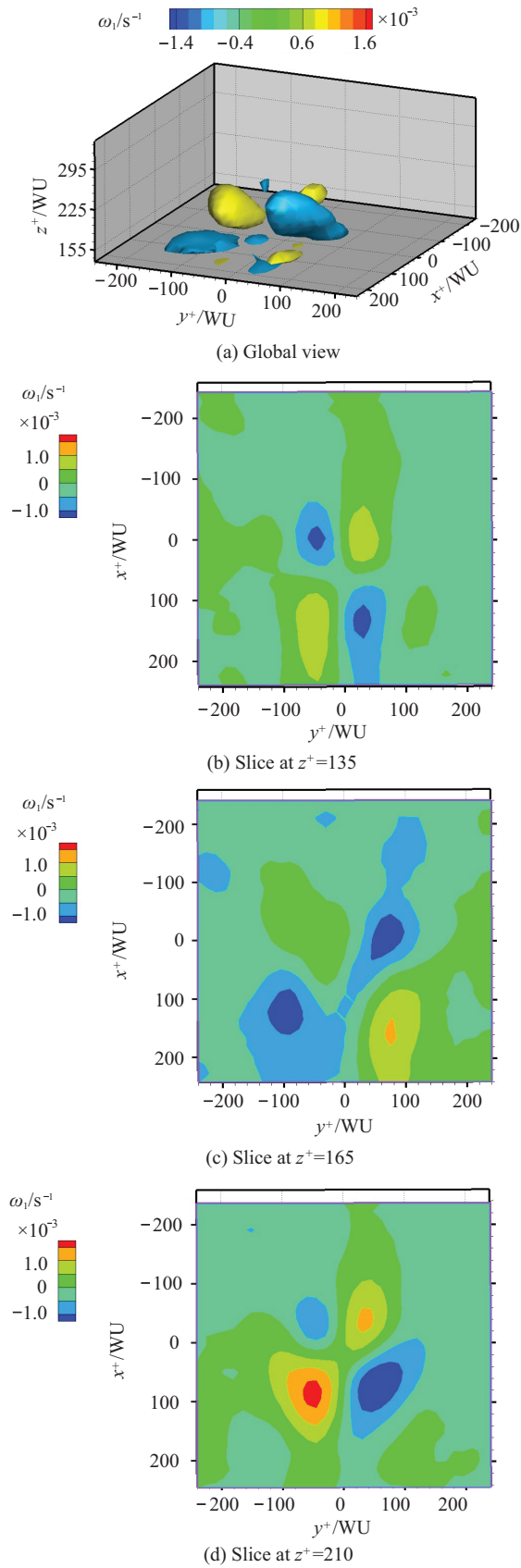


Fig. 3. The quadrupole vortex packet of streamwise vorticity component ω_1 in the different planes parallel to the wall.

antisymmetric quadrupoles in the logarithmic layer. In details, we selected three slices parallel to the wall at $z^+=135$ (Fig. 3(b)), $z^+=165$ (Fig. 3(c)), and $z^+=210$ (Fig. 3(d)). Each of the three slices corresponds to an antisymmetric quadrupoles. In these slices, each quadrupole structure consists of two pairs of counter-rotating vortex with antisymmetric layout with the neighbored vorticities have opposite signs in all streamwise, spanwise, and wall-normal directions. It implies that the near-wall layer and the outer layer of the logarithmic layer are not absolutely separated but in a close relationship.

In Fig. 4(a), an antisymmetric quadrupole structure be found from the contour of wall-normal vorticity component ω_3 in near-wall layer with two pairs of counter-rotating ω_3 as well. The position of the two pairs of ω_3 is in accordance with that of ω_1 in the near-wall region in Fig. 3(b).

To verify whether the antisymmetric quadrupole is a universal topological mode in the TBL, the spatial isosurfaces of velocity strain rates and velocity gradients were presented in Figs. 4(b) and 4(c) as well. These results show the same antisymmetric characteristics as that of ω_3 component in Fig. 4(a).

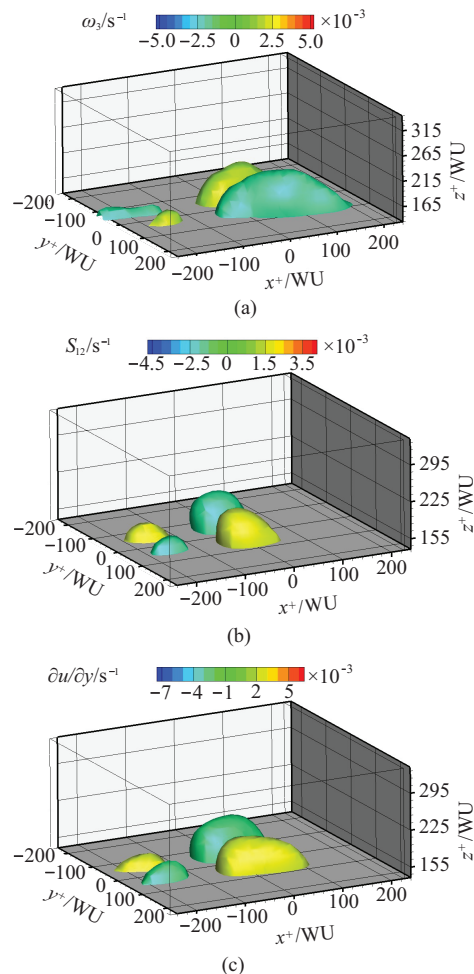


Fig. 4. Iso-surface contours of antisymmetric quadrupole topological mode for (a) ω_3 , (b) S_{12} , and (c) $\partial u/\partial y$.

Connecting the topological mode of wall-normal vortex ω_3 in Fig. 4(a), velocity strain rates S_{12} in Fig. 4(b), and velocity gradients $\partial u/\partial y$ in Fig. 4(c), the influenced regions by ejection are all below $z^+=205$. These show that vortices below $z^+=205$ must have an inclined angle since they have two vorticity components ω_1 (as shown in Fig. 3(a)) and ω_3 (as shown in Fig. 4(a)). The two pairs of counter-rotating streamwise vortices near $z^+=135$ and the other two pairs vortices near $z^+=165$ played the key role in the burst of coherent structures.

The letter presents several new experimental results about the antisymmetric quadrupole vortex packet of coherent structure bursts in the logarithmic flow by Tomo-TRPIV measurement in wall-bounded turbulence and the following conclusions are obtained.

(1) In the wall-bounded turbulence, the multi-scale characteristics of spatial deformation and rotation in vortex structures can be well described by the spatial locally averaged velocity structure function.

(2) The spatial antisymmetric quadrupole modes for velocity gradients, strain rates and the vorticities in the wall-bounded turbulence were observed for the first time by the Tomo-TRPIV system. The antisymmetric quadrupoles were proved to be universal modes for velocity gradients, vorticities and velocity strain rates of coherent structure bursts.

(3) A large-scale vortex packet was composed of three layers of quadrupoles for the ejection events.

For each quadrupole structure, there are two pairs of counter-rotating vortices with antisymmetric layout. In the logarithmic layer of the wall-bounded turbulence, the near-wall layer and the outer layer are in a close relationship.

The authors sincerely thank the experimental team in TU Delft and the German Aerospace Center (DLR) for providing the Tomographic TRPIV dataset. This work was supported by the National Natural Science Foundation of China (11272233), National Basic Research Program (973 Program) (2012CB720101), and 2013 Opening Fund of LNM, Institute of Mechanics, Chinese Academy of Sciences.

1. S. J. Kline, W. C. Reynolds, F. H. Schraub, et al., *J. Fluid Mech.* **30**, 741 (1967).
2. N. Jiang and J. Zhang, *Chin. Phys. Lett.* **22**, 1968 (2005).
3. R. E. Falco, *Phys. Fluids* **20**, S124 (1977).
4. M. R. Head and P. Bandyopadhyay, *J. Fluid Mech.* **107**, 297 (1981).
5. P. Moin and J. Kim, *J. Fluid Mech.* **155**, 441 (1985).
6. R. J. Adrian, C. D. Meinhart, and C. D. Tomkins, *J. Fluid Mech.* **422**, 1 (2000).
7. A. Schröder, R. Geisler, G. E. Elsinga, et al., *Exp. Fluids* **50**, 1071 (2011).
8. J. H. Liu, N. Jiang, and Z. D. Wang, *Appl. Math. Mech.* **26**, 495 (2005).
9. S. Q. Yang and N. Jiang, *Sci. China-Phys. Mech. Astron.* **55**, 1863 (2012).